



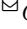


# Towards an Efficient Shifted Cholesky QR for Applications in Model Order Reduction using pyMOR

Maximilian Bindhak <sup>\*</sup>,  Art J. R. Pelling <sup>†</sup> Jens Saak <sup>\*</sup>

<sup>\*</sup> *Computational Methods in Systems and Control Theory,*  
Max Planck Institute for Dynamics of Complex Technical Systems,  
Magdeburg, Germany

<sup>†</sup> *Department of Engineering Acoustics,*  
Technische Universität Berlin, Germany

 *Corresponding author, Email: bindhak@mpi-magdeburg.mpg.de*

**Abstract:** Many model order reduction (MOR) methods rely on the computation of an orthonormal basis of a subspace onto which the large full order model is projected. Numerically, this entails the orthogonalization of a set of vectors. The nature of the MOR process imposes several requirements for the orthogonalization process. Firstly, MOR is oftentimes performed in an adaptive or iterative manner, where the quality of the reduced order model, i.e., the dimension of the reduced subspace, is decided on the fly. Therefore, it is important that the orthogonalization routine can be executed iteratively. Secondly, one possibly has to deal with high-dimensional arrays of abstract vectors that do not allow explicit access to entries, making it difficult to employ so-called ‘orthogonal triangularization algorithms’ such as Householder QR.

For these reasons, (modified) Gram-Schmidt-type algorithms are commonly used in MOR applications. These methods belong to the category of ‘triangular orthogonalization’ algorithms that do not rely on elementwise access to the vectors and can be easily updated. Recently, algorithms like shifted Cholesky QR have gained attention. These also belong to the aforementioned category and have proven their aptitude for MOR algorithms in previous studies. A key benefit of these methods is that they are communication-avoiding, leading to vastly superior performance on memory-bandwidth-limited problems and parallel or distributed architectures. This work formulates an efficient updating scheme for Cholesky QR algorithms and proposes an improved shifting strategy for highly ill-conditioned matrices.

The proposed algorithmic extensions are validated with numerical experiments on a laptop and computation server.

**Keywords:** Cholesky decomposition, QR decomposition, Cholesky QR, shifted Cholesky QR, pyMOR, benchmark, performance comparison

**Mathematics subject classification:** 65F25, 15A23, 15A12, 65F35, 68Q25, 65Y20

**Novelty statement:** Our contribution in this work is two-fold.

- We propose some algorithmic changes to the shifted Cholesky QR algorithm which improve its numerical robustness and performance in certain contexts.
- We execute a thorough performance comparison in a situation where only vector-wise access to the matrix columns is allowed.

## 1. Introduction

Mathematical modeling of complex dynamical systems oftentimes produces very large models that can become numerically infeasible in practice. The endeavor of finding smaller, and therefore more efficient, surrogate models while retaining the most important dynamics of the system is known as model order reduction (MOR) [2, 4–7]. The majority of MOR methods achieve the reduction of model size by means of projection. Hereby, the degrees of freedom (DOFs) of the full order model (FOM) are projected onto a subspace of smaller dimension. The main challenge in MOR is finding a subspace that is small, yet leads to accurate reduced order models (ROMs). These subspaces are usually represented by bases of orthonormal vectors that are constructed during the MOR process. Therefore, orthogonalization routines are required in many MOR tasks such as moment matching (MM) [18, 25], the iterative restarted Krylov algorithm (IRKA) [26], proper orthogonal decomposition (POD) [40] and also recent data-driven MOR methods such as the randomized Eigensystem Realization algorithm (rERA) [32].

The landscape of orthogonalization methods is vast and growing with many recent developments [11–13, 20]. Following the conceptualization in [21, 42], orthogonalization algorithms can be divided into so-called *orthogonal triangularization* algorithms that successively left-multiply orthogonal matrices until a triangular matrix is obtained, and *triangular orthogonalization* algorithms that multiply triangular matrices from the right until an orthogonal matrix is obtained. The former *orthogonal triangularization* methods include all Householder-type QR algorithms [9, 39], whereas Gram-Schmidt-type methods, and recently also Cholesky QR-type [21–23] algorithms, belong to the latter class of *triangular orthogonalization* methods.

Even though there are plenty of orthogonalization methods to choose from, the application at hand imposes constraints on the choice of method. In this work, we will look through the lens of MOR applications, specifically using the free and open source Python software library pyMOR [30, 36]. A special requirement of the orthogonalization methods in pyMOR is the abstract operator and `VectorArray` interface. The key idea is that the MOR process is formulated in an abstract manner whereby the construction and solution of FOMs is offloaded to established software libraries.

On the one hand, this abstraction enables easy integration of almost any arbitrary solver for partial differential equations (PDEs) because boilerplate code is largely avoided, increasing the applicability of the algorithms. Further, it allows MOR routines to be implemented such that they are independent of the concrete PDE problem and solver. Thus, the maintenance effort for the MOR code is reduced drastically and the integration of new algorithms by non-experts regarding the specific PDE

solvers is straightforward. This gives maximum flexibility to try the methods on a whole range of problems. On the other hand, tall and skinny matrices become mere arrays of vectors that reside in the PDE solver’s memory space and their concrete realization may be such that access to single degrees of freedom (DOFs) is either very expensive or even impossible. This is especially true when the PDE solver is run in distributed parallel mode and significant bookkeeping is required to identify on which of the processes, i.e., involved hosts, the required DOFs reside.

In effect, this introduces several numerical and algorithmic restrictions when dealing with large-scale problems: As the software interface has to accommodate a wide range of backends, only entire FOM solutions can be queried and single DOFs generally cannot be accessed. In consequence, *orthogonal triangularization* algorithms such as Householder-type methods can mostly be ruled out for MOR applications in pyMOR, as DOF-access is needed to construct the Householder reflectors. Also, the communication-avoiding so-called tall and skinny QR decomposition (TS-QR) [17]<sup>1</sup>, which splits the tall and skinny matrix into blocks vertically, requires DOF-access to achieve this splitting, hence cannot be implemented in terms of the present abstraction. This leaves the class of *triangular orthogonalization* methods such as Gram-Schmidt type algorithms and the Cholesky QR variants which will be considered in this work.

In a nutshell, the basic Cholesky QR algorithm relies on the observation that the QR decomposition of a matrix  $A$  can be computed from a decomposition of its Gramian  $X = A^T A$ . Namely, from a Cholesky factor  $R$  of the Gramian  $X = R^T R$ , where  $R$  is upper triangular, the QR decomposition  $A = QR$  can be obtained by  $Q = AR^{-1}$ . Of course, this simple relationship only holds in exact arithmetic and this basic algorithm is unstable in practice. Several algorithmic extensions [21–23] of the basic algorithm have been proposed recently that solve the issue of numerical instability.

For QR decompositions in MOR applications, we can generally distinguish two modes of operation:

- M1 In algorithms like IRKA [26], or when truncating the rank of the system Gramians in balancing-based MOR [37], one obtains the entire non-orthonormal bases and run a full QR sweep all-at-once. Here, comparably many columns at a time are being orthonormalized and approaches based on Cholesky QR are well-suited.
- M2 In adaptive approaches, such as MM with a posteriori error estimates [15], adaptive data-driven modeling [35], or in POD-Greedy approaches, like the reduced basis (RB) method [6], we successively increase the number of basis vectors. That means, one

<sup>1</sup>An extensive comparison between TS-QR with the repeated Cholesky QR was done in [23], which shows significant speedups for the latter on parallel distributed systems.

extends an existing orthonormal basis by one or more new vectors that still need orthonormalization. In other words, one performs a QR update. Especially in POD/RB-like approaches, it then often happens that less and less of the new vectors are actually sufficiently linearly independent of the existing basis, i.e., the condition number of the full matrix of basis vectors becomes increasingly large. Usually, Gram-Schmidt-type approaches are then used, as they allow detection of the linear dependence and vectors can be dropped accordingly. However, this detection may only happen after comparison to many previously computed orthonormal vectors, causing significant communication (memory movements) overhead. In this work, we argue that Cholesky QR-type algorithms can be computationally advantageous in this mode of operation as well.

In both cases, the classic Cholesky QR algorithm [24, Theorem 5.2.3] suffers from a potential linear dependence of basis vectors, as the computation of the Gramian squares the conditioning of the problem and very ill-conditioned matrices can enter the Cholesky decomposition. The shifted Cholesky QR [21, 23] is a remedy to this issue, but it can become slow when the shift needs to be repeated very often or, as demonstrated later, might outright fail. Moreover, in pyMOR’s abstraction, the Gramian computation can be executed as a BLAS level-3-type GEMM operation only for `NumpyVectorArrays`<sup>2</sup> and is limited to a single inner product of two vectors, i.e., strictly BLAS level-1 per entry of the Gramian, for generic `VectorArrays` such as `ListVectorArray`<sup>3</sup> and others.

In this contribution, we tackle both issues. To this end, we suggest three algorithmic extensions in Section 2. An evaluation of the required number of floating point operations of the corresponding algorithms can be found in Appendix A. Section 3 presents an extensive performance evaluation benchmarking the algorithms with respect to execution time and several accuracy measures. This illustrates the numerical robustness of the newly proposed algorithmic extensions for a variety of input matrices. In Section 4, we conclude the paper and discuss possible further extensions and investigations.

## 2. Extensions of the Shifted Cholesky QR Algorithm

Above, we have identified two main issues with the shifted Cholesky QR. In this section, we provide a remedy for the potential breakdowns or expensive inner loops in the presence of linearly dependent vectors, due to ill-conditioned

or very large Gramians  $X = A^T A$ . We address the ill-conditioning by adapting the shift in Section 2.1.

As mode M2 mostly relies on QR updates, we propose an efficient updating scheme for “Cholesky QR”-type decompositions. This is finally used in Section 2.3 to devise a panel scheme that successively computes updated QR decompositions with a block of columns added in each step. This improves the operations count and the memory locality of the procedure when using pyMOR’s `VectorArray` abstraction and ultimately limits the dimensions of the Gramian.

### 2.1. Shift recomputation

As is supported by the numerical experiments in Sections 3.2 and 3.3, we now propose a more numerically robust variation of the ‘*Iterated Cholesky QR for  $X = QR$  with shifts when necessary*’ algorithm presented in [21, Algorithm 4.1]<sup>4</sup> (ITER-SCHOLQR). Experiments have shown that, in very ill-conditioned cases, the ITER-SCHOLQR does not converge to an orthogonal  $Q$  because the initial shift estimation based on  $\|A\|_2^2$  is too large by orders of magnitude. This large shift is then reapplied in successive iterations, ultimately producing a non-orthogonal  $Q$ . A straightforward solution to this problem is to simply recompute the shift according to the current approximation. To this end, we present the ‘*Iterated Cholesky QR with shift recomputation*’ (RSCHOLQR) in Algorithm 1 that, rather than reapplying the initial shift, recomputes the shift whenever the Cholesky decomposition of the current Gramian iterate  $X$  fails. Since  $\|X\|_2 = \|A\|_2^2$ , we propose to compute the shift based on  $\|X\|_2$ . Not only does this solve the problem of a non-orthogonal  $Q$  because the shift matches the current iterate, it can further be numerically more efficient: Despite performing shift computations repeatedly instead of only once, multiple computations of  $\|X\|_2$  can be less expensive than  $\|A\|_2^2$ , depending on the dimension of  $A$  and number of required iterations. Furthermore, one can utilize symmetric eigenvalue solvers, like the Lanczos method [27] or implicitly restarted Lanczos method (IRLM) [41], to compute only the largest eigenvalue of the Gramian  $X$  because it is symmetric/hermitian.

It is important to note that, in certain instances, it is possible that the shift becomes insignificantly small in later iterations and the proposed algorithm ends up in a quasi-infinite loop. As a remedy, it is advised to limit the magnitude of the shift by twice the unit round-off from below (Line 6 in Algorithm 1).

In order to get an impression of possible savings from this extension, as well as the extensions introduced in the following subsections, we collect the required floating point operations (flops) in Table 4, found in Appendix A.

<sup>2</sup><https://docs.pymor.org/2024-2-0/autoapi/pymor/vectorarrays/numpy/index.html>

<sup>3</sup><https://docs.pymor.org/2024-2-0/autoapi/pymor/vectorarrays/list/index.html>

<sup>4</sup>Note that the naming scheme for  $X$  and  $A$  in [21] is exactly opposite to the scheme used in this paper.

**Algorithm 1** (rsCHOLQR): Iterated Cholesky QR with shift recomputation.

**Input:**  $A \in \mathbb{R}^{m \times n}$ , unit roundoff  $\mathbf{u} > 0$ .

**Output:**  $Q \in \mathbb{R}^{m \times n}$ ,  $R \in \mathbb{R}^{n \times n}$

```

1:  $Q \leftarrow A$ 
2:  $R \leftarrow I_n$ 
3:  $X \leftarrow Q^T Q$ 
4: while  $\|X - I_n\|_F \geq \mathbf{u}\sqrt{n}$  do
5:   if  $\tilde{R} \leftarrow \text{chol}(X)$  breaks down then
6:      $\sigma \leftarrow \max \{11(mn + n(n+1))\mathbf{u} \|X\|_2, 2\mathbf{u}\}$   $\triangleright$ 
       Recompute shift.
7:      $\tilde{R} \leftarrow \text{chol}(X + \sigma I_n)$ 
8:   end if
9:    $Q \leftarrow Q \tilde{R}^{-1}$ 
10:   $R \leftarrow \tilde{R} R$ 
11:   $X \leftarrow Q^T Q$ 
12: end while
```

Note that especially the `xGEMM`<sup>5</sup> operations for forming the Gramians are not memory traffic optimal due to the pyMOR abstraction, such that direct comparison with NumPy's `numpy.ndarray` will favor the latter due to its better memory management.

## 2.2. Updating the decomposition

As mentioned in Section 1, many adaptive MOR tasks require a repeated orthonormalization to extend an existing orthonormal basis with new vectors (operation mode M2). To this end, we formulate a QR-updating scheme for the (shifted) Cholesky QR algorithm in Algorithm 2. The core algorithm was recently presented for a data-driven MOR application by the second author in [35, Appendix A]. In this work, it is analyzed indirectly via the panel variant introduced in Section 2.3 with respect to its numerical behavior and careful benchmarking against the existing approaches applicable in pyMOR is undertaken.

Suppose we have an existing QR decomposition

$$Q_1 R_1 = A_1 \in \mathbb{R}^{m \times q}$$

and are looking to obtain a QR decomposition for an updated matrix  $A = \begin{bmatrix} A_1 & A_2 \end{bmatrix}$ , i.e., find  $Q_2, B, R_2$  such that

$$Q = \begin{bmatrix} Q_1 & Q_2 \end{bmatrix} \in \mathbb{R}^{m \times (q+p)}$$

and

$$R = \begin{bmatrix} R_1 & B \\ 0 & R_2 \end{bmatrix} \in \mathbb{R}^{(q+p) \times (q+p)}.$$

$A_2 \in \mathbb{R}^{m \times p}$  denotes the new columns that have been appended to  $A_1$ , where  $Q_2$  is its orthogonalization with re-

spect to  $Q_1$ . The following proposition reveals how an updated QR decomposition can be obtained from a Cholesky approach:

**Proposition 2.1.** *Let  $Q_1 \in \mathbb{R}^{m \times q}$ ,  $R_1 \in \mathbb{R}^{q \times q}$  be a QR decomposition  $Q_1 R_1 = A_1 \in \mathbb{R}^{m \times q}$  and let  $R_2$  be given by the Cholesky factorization*

$$\begin{aligned} R_2^T R_2 &= (A_2 - Q_1 Q_1^T A_2)^T (A_2 - Q_1 Q_1^T A_2) \\ &= A_2^T A_2 - A_2^T Q_1 Q_1^T A_2 = X \end{aligned}$$

for some  $A_2 \in \mathbb{R}^{m \times p}$ . Then,

$$Q = \begin{bmatrix} Q_1 & (A_2 - Q_1 Q_1^T A_2) R_2^{-1} \end{bmatrix}$$

and

$$R = \begin{bmatrix} R_1 & Q_1^T A_2 \\ 0 & R_2 \end{bmatrix}$$

is a QR decomposition of  $A = \begin{bmatrix} A_1 & A_2 \end{bmatrix} \in \mathbb{R}^{m \times (q+p)}$ .

*Proof.* Firstly, we have

$$\begin{aligned} QR &= \begin{bmatrix} Q_1 R_1 & Q_1 Q_1^T A_2 + (A_2 - Q_1 Q_1^T A_2) R_2^{-1} R_2 \end{bmatrix} \\ &= \begin{bmatrix} A_1 & A_2 \end{bmatrix} = A. \end{aligned}$$

Secondly,  $R$  is upper triangular by construction.

It remains to verify that  $Q$  is orthogonal. Let

$$Q_2 = (A_2 - Q_1 Q_1^T A_2) R_2^{-1},$$

such that

$$Q = \begin{bmatrix} Q_1 & (A_2 - Q_1 Q_1^T A_2) R_2^{-1} \end{bmatrix}.$$

Then,

$$\begin{aligned} Q_1^T Q_2 &= Q_1^T (A_2 - Q_1 Q_1^T A_2) R_2^{-1} \\ &= (Q_1^T A_2 - Q_1^T A_2) R_2^{-1} = 0, \end{aligned}$$

and

$$\begin{aligned} Q_2^T Q_2 &= R_2^{-T} (A_2 - Q_1 Q_1^T A_2)^T (A_2 - Q_1 Q_1^T A_2) R_2^{-1} \\ &= R_2^{-T} (R_2^T R_2) R_2^{-1} = I_p. \end{aligned}$$

Thus,  $Q^T Q = I_{q+p}$ .  $\square$

The computation of the Cholesky factor  $R_2$  can be stabilized by applying shifts whenever it breaks down, just as it is done in Algorithm 1. Multiple iterations might be necessary to reach the desired accuracy. However, also breakdowns can happen, although they are lucky breakdowns, as we will explain in the following. To this end, we consider two columns  $a_i$  and  $c_j$  of  $A_2$  with  $a_i$  being a linear combination of vectors in  $Q_1$ , i.e.,  $a_i = Q_1 b_i$  for

<sup>5</sup>Here, `xGEMM` refers to a general matrix-matrix product from BLAS, which is usually associated with a highly parallelizable operation. More operations in BLAS/LAPACK notation used in this paper can be found in Table 3.

some  $b_i \in \mathbb{R}^q$  and  $c_j$  orthogonal on  $Q_1$ , i.e.,  $Q_2^\top c_j = 0$ . Then, we have

$$\begin{aligned} X_{i,i} &= a_i^\top a_i - a_i^\top Q_1 Q_1^\top a_i \\ &= b_i^\top Q_1^\top Q_1 b_i - b_i^\top b_i = 0. \end{aligned}$$

Clearly, this leads to a rank deficiency in the Gramian (as Sylvester's criterion is violated, and definiteness is lost) and the Cholesky decomposition will fail. However, in MOR, one is usually interested in a rank revealing QR decomposition and one could simply proceed with the reduced Gramian formed without  $a_i$ . On the other hand,

$$\begin{aligned} X_{j,j} &= c_j^\top c_j - \underbrace{c_j^\top Q_1 Q_1^\top c_j}_{=0} \\ &= c_j^\top c_j. \end{aligned}$$

In practice, obviously anything in between can happen and  $X$  can be arbitrarily ill-conditioned. To avoid issues with the Cholesky decomposition of  $X$ , we resort to shifting in this contribution. However, a suitable combination of shifting and a column pivoting strategy along the lines of [22] could potentially yield even better results.

The considerations made above also apply to the panel scheme devised in the next section when successively updating existing QR decompositions. Especially there, the initial shift is often by magnitudes too small. Our current workaround is to increase it by a factor of 10 until the shifted Cholesky decomposition succeeds. We have experimented with different strategies, but have not found any that has similar robustness at lower computational costs, yet. In any case, we have observed runtime improvements even with this rather brute force approach, as reported in Section 3 and [35].

### 2.3. A panel scheme

We introduce a straightforward QR panel scheme based on CHOLQRUPDATE from Algorithm 2. The main goal of this approach are runtime improvements. The idea is to split the input matrix  $A$  into  $r$  (ideally) equally sized panels  $A = [A_1 \ A_2 \ \dots \ A_r]$  and apply CHOLQRUPDATE iteratively onto these panels. This scheme reduces the size of the Gramian per iteration, allowing for a cheaper Cholesky decomposition and shift evaluation, especially if  $X$  is small enough to fit into the lower cache levels. In Appendix A.1, we analyze the operation counts and show a theoretical decrease in flops by a factor of up to two for an increasing amount of panels compared to RSCHOLQR. This can potentially also lead to a reduction in power consumption. The pseudocode for this procedure can be found in Algorithm 3.

However, the reduction of flops does not necessarily result in a decrease in runtime, as will be illustrated in Section 3.4. Unlike, for example, the level-3-type LAPACK implementations of the LU (xGETRF) and QR de-

---

#### Algorithm 2 (CHOLQRUPDATE):

---

**Input:** Existing QR decomposition  $Q_1 \in \mathbb{R}^{m \times q}$ ,  $R_1 \in \mathbb{R}^{q \times q}$ , new columns  $A_2 \in \mathbb{R}^{m \times p}$ , unit roundoff  $\mathbf{u} > 0$ .  
**Output:**  $Q \in \mathbb{R}^{m \times n}$ ,  $R \in \mathbb{R}^{n \times n}$  that satisfies  $q + p = n$  and  $QR = [Q_1 R_1 \ A_2]$ .

```

1:  $Q_2 \leftarrow A_2$ 
2:  $B \leftarrow 0 \in \mathbb{R}^{q \times p}$ 
3:  $R_2 \leftarrow I_p$ 
4:  $\tilde{B} \leftarrow Q_1^\top Q_2$ 
5:  $X \leftarrow Q_2^\top Q_2 - \tilde{B}^\top \tilde{B}$ 
6: while  $\|X - I_p\|_F \geq \mathbf{u}\sqrt{p}$  do
7:    $\sigma \leftarrow 0$ 
8:   while  $\tilde{R} \leftarrow \text{chol}(X + \sigma \cdot I_p)$  breaks down do
9:      $\sigma \leftarrow \begin{cases} 11(mq + q(q+1))\mathbf{u}\|X\|_2 & \sigma = 0 \\ 10 \cdot \sigma & \text{else} \end{cases}$ 
10:     $\sigma \leftarrow \max\{\sigma, 2\mathbf{u}\}$ 
11:   end while
12:    $Q_2 \leftarrow (Q_2 - Q_1 \tilde{B}) \tilde{R}^{-1}$ 
13:    $B \leftarrow B + \tilde{B} R_2$ 
14:    $R_2 \leftarrow \tilde{R} R_2$ 
15:    $\tilde{B} \leftarrow Q_1^\top Q_2$   $\triangleright$  Update  $\tilde{B}$  for next iteration.
16:    $X \leftarrow Q_2^\top Q_2 - \tilde{B}^\top \tilde{B}$   $\triangleright$  Update  $X$  for next iteration.
17: end while
18:  $Q \leftarrow [Q_1 \ Q_2]$ 
19:  $R \leftarrow \begin{bmatrix} R_1 & B \\ 0 & R_2 \end{bmatrix}$ 
```

---

composition (xGEQRF + x(OR/UN)GQR), which replace several BLAS level-1-type and level-2-type calls with level-3-type routines on the full matrix, PNCHOLQR(R) only introduces more level-3-type calls with smaller Gramian matrices depending on the size of the panels. However, the aforementioned issues with CHOLQRUPDATE persist as the algorithm cannot act cleverly in the large direction ( $m$ ). In other words, we admittedly cannot avoid the large direction, but we can control the size of the Gramians and the data traffic required for forming them and computing with them. At the same time, lower level caches get increasingly exclusive to single cores or core groups, limiting the parallelism in the computations. The latter being especially harmful for systems with many cores, as we will see in Section 3. Moreover, we observed fewer repetitions are required to evaluate the QR decomposition of the first few panels, but it becomes successively more expensive for the later panels due to the higher probability/fraction of linear dependence.

## 3. Benchmarks

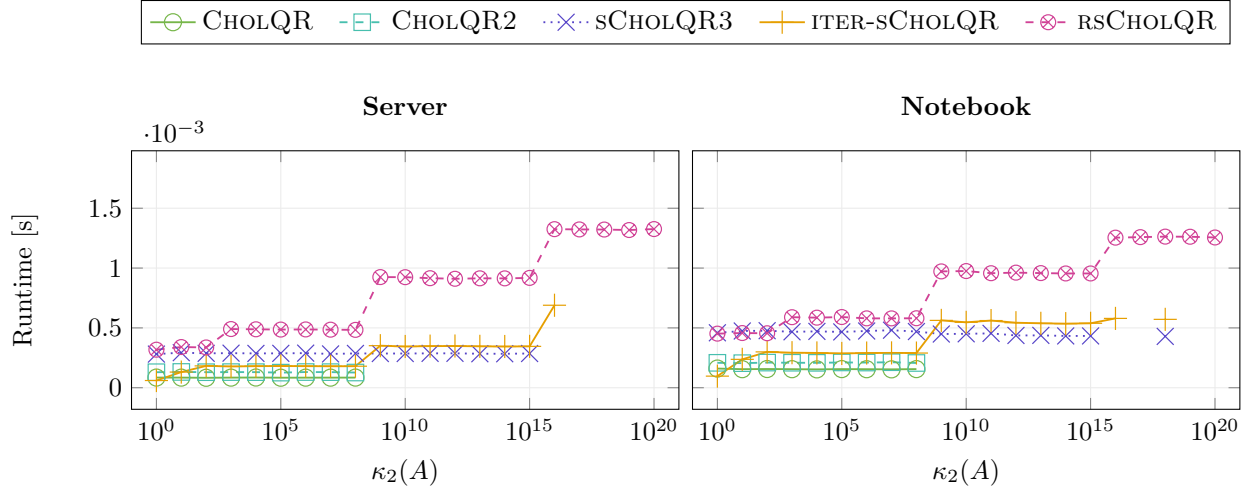
In the following we introduce our test framework and evaluate our numerical experiments. First, we specify the

	Server	Notebook
Operating system	Ubuntu 20.04.6 LTS	Ubuntu 24.04.2 LTS
Conda version	25.3.0	24.5.0
Main memory size	$\approx 1$ TB	16 GB
CPU	2x AMD EPYC™ 7763	AMD Ryzen™ 7730U
CPU architecture	Zen™ 3	Zen™ 4
Number physical cores (logical)	64 (128)	8 (16)
L3 cache per 8 cores (CPU total)	32 MB (256 MB)	16 MB (16 MB)
L2 cache per core (CPU total)	512 KB (32.768 MB)	512 KB (4.096 MB)
L1 instructions cache per core (CPU total)	32 KB (2.048 MB)	32 KB (0.256 MB)
L1 data cache per core (CPU total)	32 KB (2.048 MB)	32 KB (0.256 MB)

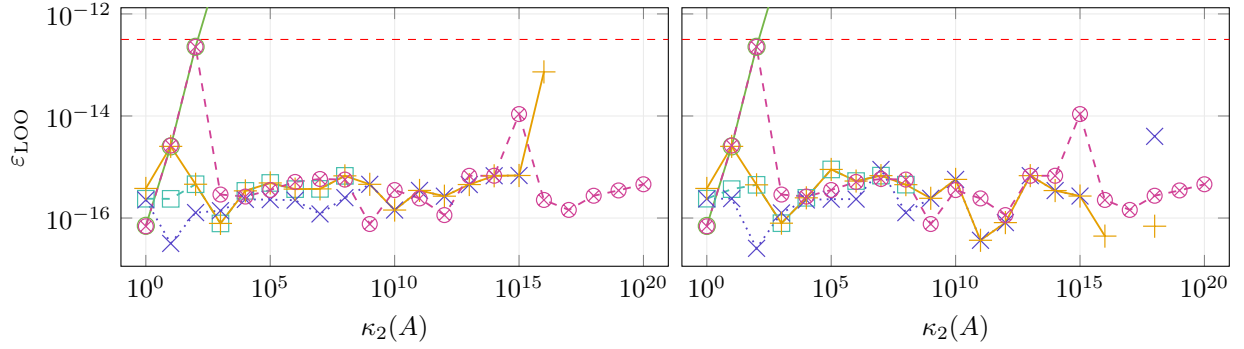
Table 1: Overview of the operating systems and hardware for the two systems used for benchmarking. Server has two CPU sockets, but only the first CPU was used ( $\approx 500$  GB RAM).

	Main Environment	FEniCS Environment
Package	Version	Version
OpenBLAS [34]	0.3.21	0.3.29
Python	3.10.17	3.12.10
NumPy [14]	1.24.4	1.26.4
SciPy [43]	1.10.1	1.15.2
pyMOR [19]	2024.2.0	2024.2.0
NGSolve [33, 38]	6.2.2501	n.a.
FEniCS [1, 29]	n.a.	2019.1.0

Table 2: Software packages used are installed via conda. Only the most important software package versions are listed in this table. For all installed packages and their respective versions, please refer to the provided YAML file.



(a) Runtime measurements. rsCHOLQR has a higher overhead due to the *pyMOR* abstraction layer. Its runtime increases for higher matrix condition numbers  $\kappa_2(A)$  due to more iterations and shifts being required to achieve orthogonality.



(b) Loss of orthogonality  $\varepsilon_{\text{LOO}}(Q) = \|I - Q^T Q\|_2$ .

Figure 1: Comparison of QR decomposition methods for  $A \in \mathbb{R}^{300 \times 10}$  and varying condition numbers  $\kappa_2(A) = 10^x$ ,  $x \in [0, 1, \dots, 20]$ , 50 repetitions. CHOLQR and CHOLQR2 fail to compute the Cholesky decomposition for  $\kappa_2(A) > 10^8$ . The same occurs for sCHOLQR3 and ITER-sCHOLQR for  $\kappa_2(A) \gtrsim 10^{16}$ . rsCHOLQR is numerical robust for the given benchmark.

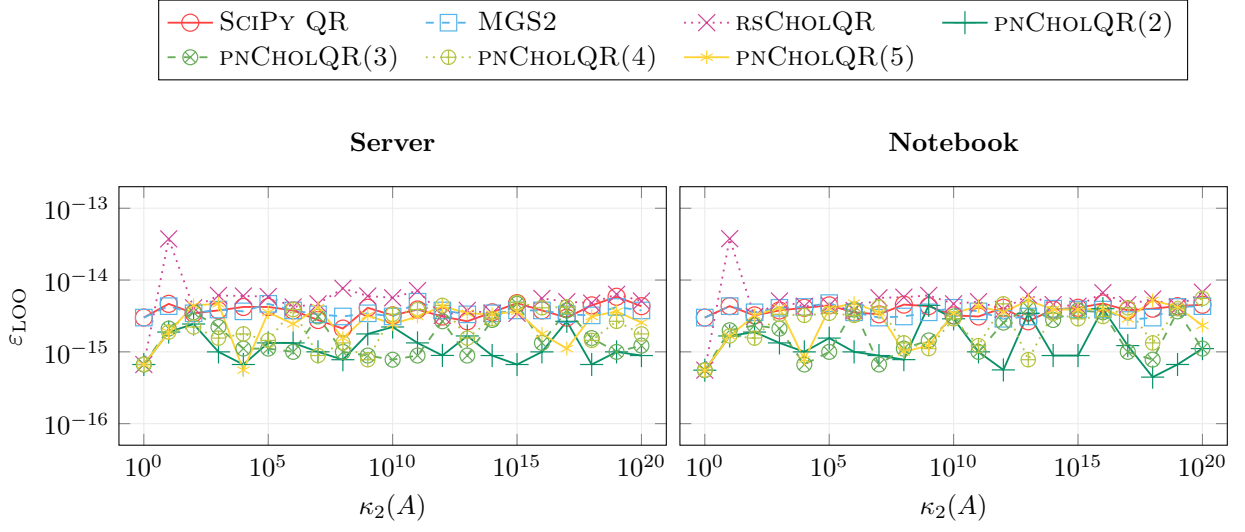
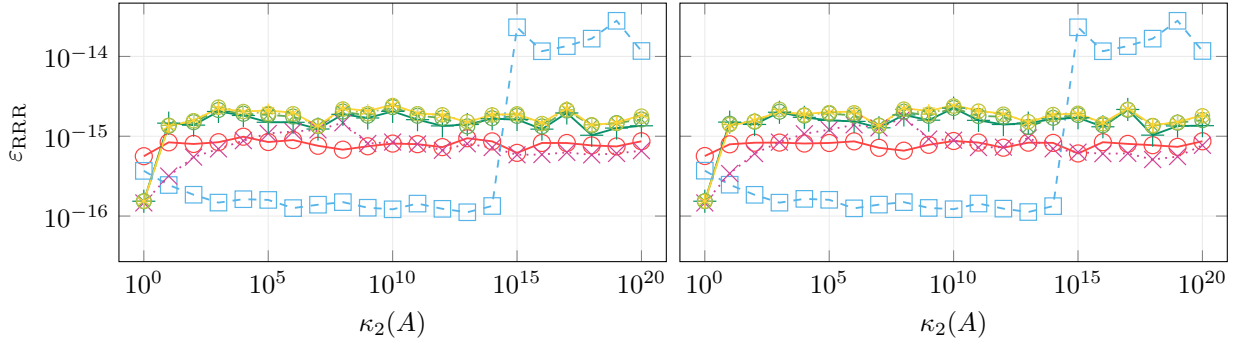
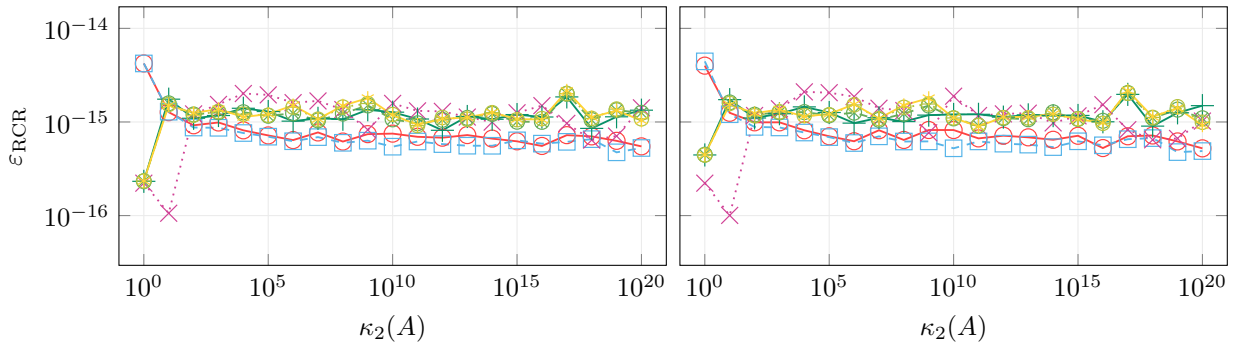
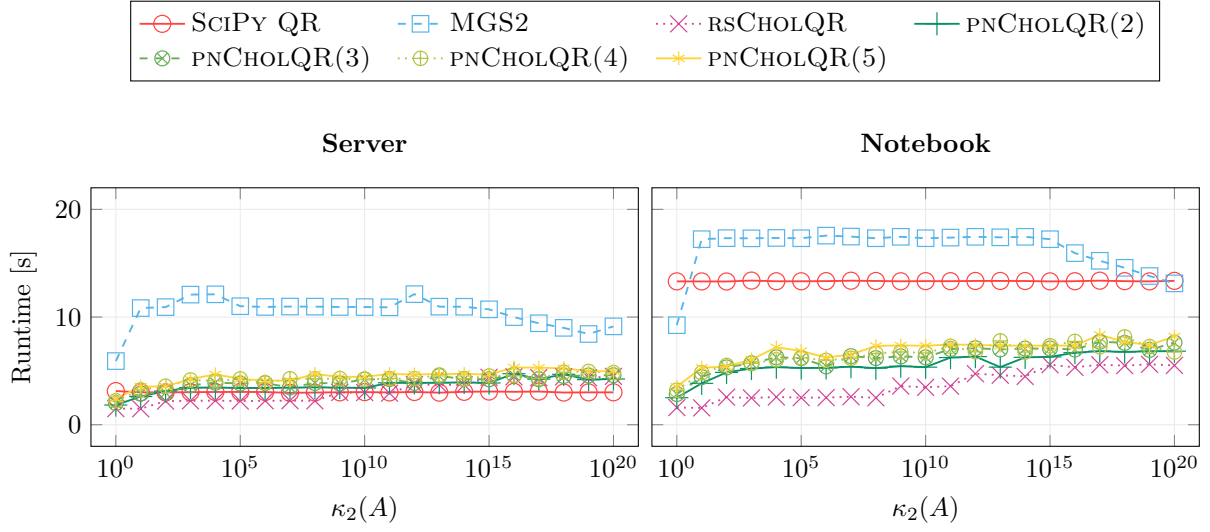
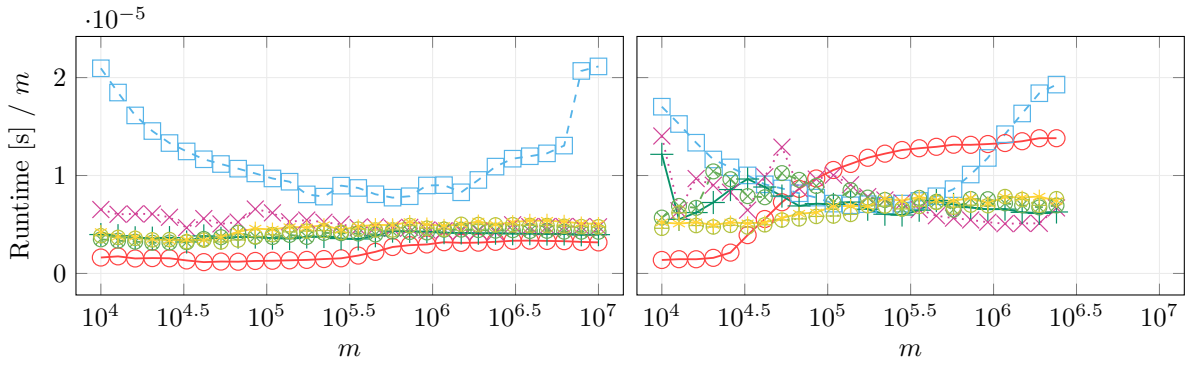
(a) Loss of orthogonality  $\varepsilon_{\text{LOO}}(Q) = \|I - Q^T Q\|_2$ .(b) Relative reconstruction residual  $\varepsilon_{\text{RRR}}(A, Q, R) = \frac{\|A - QR\|_2}{\|A\|_2}$ .(c) Relative Cholesky residual  $\varepsilon_{\text{RCR}}(A, R) = \frac{\|A^T A - R^T R\|_2}{\|A\|_2^2}$ .

Figure 2: QR quality measures over varying matrix condition number of a matrix  $A \in \mathbb{R}^{10^6 \times 100}$  and condition numbers  $\kappa_2(A) = 10^x$ ,  $x \in [0, 1, \dots, 20]$ , 10 repetitions. Due to the rank-revealing features of MGS2, its relative reconstruction residual  $\varepsilon_{\text{RRR}}$  increases for  $\kappa_2(A) \geq 10^{15}$ . All algorithms provide good solutions and do not fail.

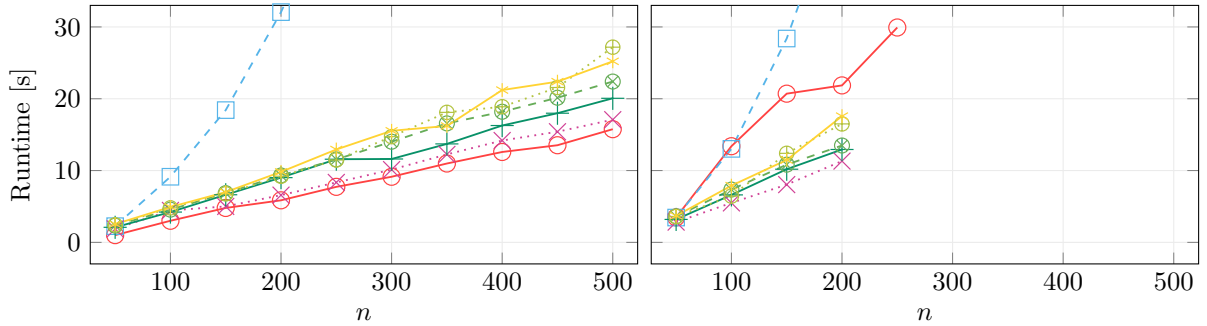




(a) Runtime over varying matrix condition number  $\kappa_2(A)$ ,  $A \in \mathbb{R}^{10^6 \times 100}$ ,  $\kappa_2(A) = 10^x$ ,  $x \in [0, 1, \dots, 20]$ .



(b) Relative runtime  $\frac{\text{runtime}}{m}$  over varying vector length  $m$ ,  $A \in \mathbb{R}^{m \times 100}$ ,  $m \in [10^4, \dots, 10^7]$ ,  $\kappa_2(A) = 10^{20}$ . The notebook is unable to compute the QR decompositions for  $m \geq 10^{6.48}$  due to memory limitations.



(c) Runtime over varying number of columns  $n$ ,  $A \in \mathbb{R}^{10^6 \times n}$ ,  $n \in [50, 100, \dots, 500]$ ,  $\kappa_2(A) = 10^{20}$ . The notebook is unable to compute the QR decompositions for  $n \geq 250$  due to memory limitations.

Figure 3: Runtime comparison by variation of different aspects of the original matrix  $A$  with 10 repetitions.

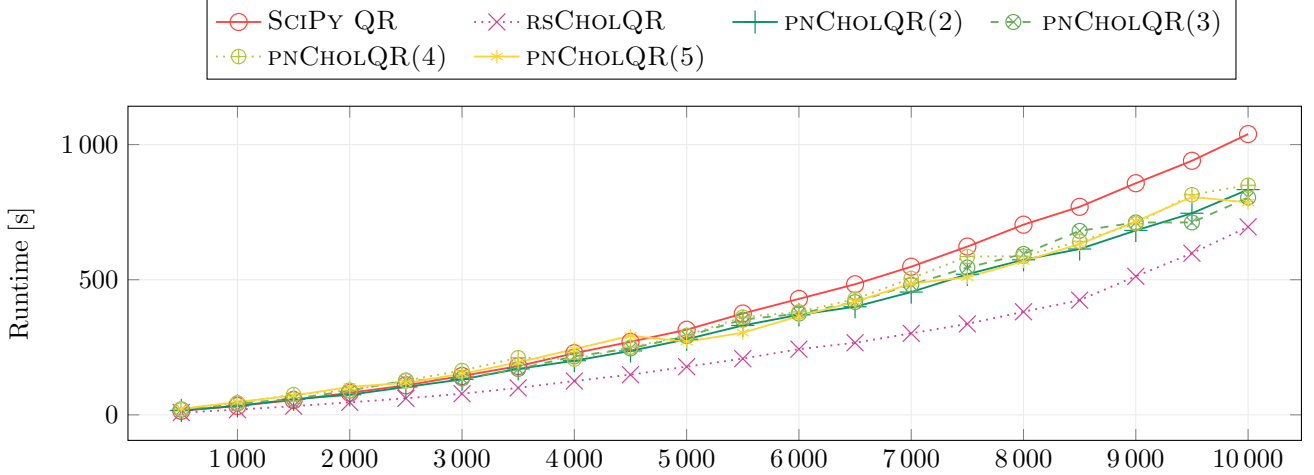


Figure 4: Runtime over varying number of columns  $n$  with 3 repetitions,  $A \in \mathbb{R}^{10^6 \times n}$ ,  $n \in [500, 1000, \dots, 10000]$ ,  $\kappa_2(A) = 10^5$ .

**Algorithm 3** (PNCHOLQR(R)): Cholesky QR panel scheme.

**Input:**  $A = \begin{bmatrix} A_1 & A_2 & \dots & A_r \end{bmatrix} \in \mathbb{R}^{m \times n}$ , unit roundoff  $u > 0$

**Output:**  $Q \in \mathbb{R}^{m \times n}$ ,  $R \in \mathbb{R}^{n \times n}$

- 1:  $Q \leftarrow \begin{bmatrix} I \\ 0 \end{bmatrix}$ ,  $R \leftarrow \begin{bmatrix} 0 \\ 0 \end{bmatrix}$
- 2: **for**  $i = 1, 2, \dots, r$  **do**
- 3:    $Q, R \leftarrow \text{CHOLQRUPDATE}(Q, R, A_i, u)$
- 4: **end for**

used computer systems, our reproducible software environments, the tested algorithms, our test matrix construction and the metrics we evaluated. Afterwards, we compare the newly introduced RSCHOLQR to already existing Cholesky QR variants, before illustrating the numerical robustness of RSCHOLQR and PNCHOLQR(R). Lastly, we show our runtime measurements for a variety of aspects of the input matrix  $A$  and the used **VectorArray** backend.

### 3.1. Implementation and test environment

The benchmark runs are executed on two systems. The system details for both are listed in Table 1. The Server system has two CPU sockets, i.e., two NUMA<sup>6</sup> nodes. For our experiments, only the first CPU was used – via node pinning using `sched.setaffinity` from the Linux kernel’s scheduler instructions – to ensure uniform memory access. Therefore, only up to 64 physical cores and 500 GB RAM can be used. On both systems logical (hyperthreading) cores are allowed. We use both a server and notebook to demonstrate how the performance of the algorithms is affected by hardware capabilities.

<sup>6</sup>[https://en.wikipedia.org/wiki/Non-uniform\\_memory\\_access](https://en.wikipedia.org/wiki/Non-uniform_memory_access)

We faced difficulties creating one single reproducible Python environment that is able to run the algorithms for all chosen **VectorArray** backends without performance degradation of the algorithms. Therefore, we decided to use two separate conda [16] environments. All shown measurements were created using the environment Main except for the measurements with the FEniCS backend, i.e., the **FEniCSListVectorArray** which were taken with the FEniCS environment. An overview of the most important software package versions can be found in Table 2. The full conda environment specifications can be found as YAML files in our **code & data repository on Zenodo** [8] and can easily be installed using Miniforge [31] and the **conda-forge** channel.

We are comparing the new algorithms with a number of similar algorithms from the literature. The algorithms are all implemented in Python using the NumPy and SciPy packages as well as pyMOR [30, 36]. The following algorithms are used in our benchmarks:

1. CHOLQR and CHOLQR2 [23] represent the simple and repeated Cholesky QR algorithms, respectively.
2. Moreover, we used ‘*shiftedCholeskyQR3 for  $X = QR$* ’ [21, Algorithm 4.2]<sup>7</sup> (SCHOLQR3) and ITER-SCHOLQR, which was previously introduced in Section 2.1. SCHOLQR3 applies a shift followed by three Cholesky QR iterations. ITER-SCHOLQR on the other hand applies a shift, which is evaluated just once, whenever a Cholesky decomposition fails and performs as many iterations as required to achieve orthogonality. Here, we have limited the number of iterations to 10.
3. Furthermore, we used the `qr` routine from SciPy, more precisely `scipy.linalg` (SciPy QR), which

<sup>7</sup>Note again, in [21] the naming scheme for  $X$  and  $A$  is exactly opposite to the scheme used in this paper.

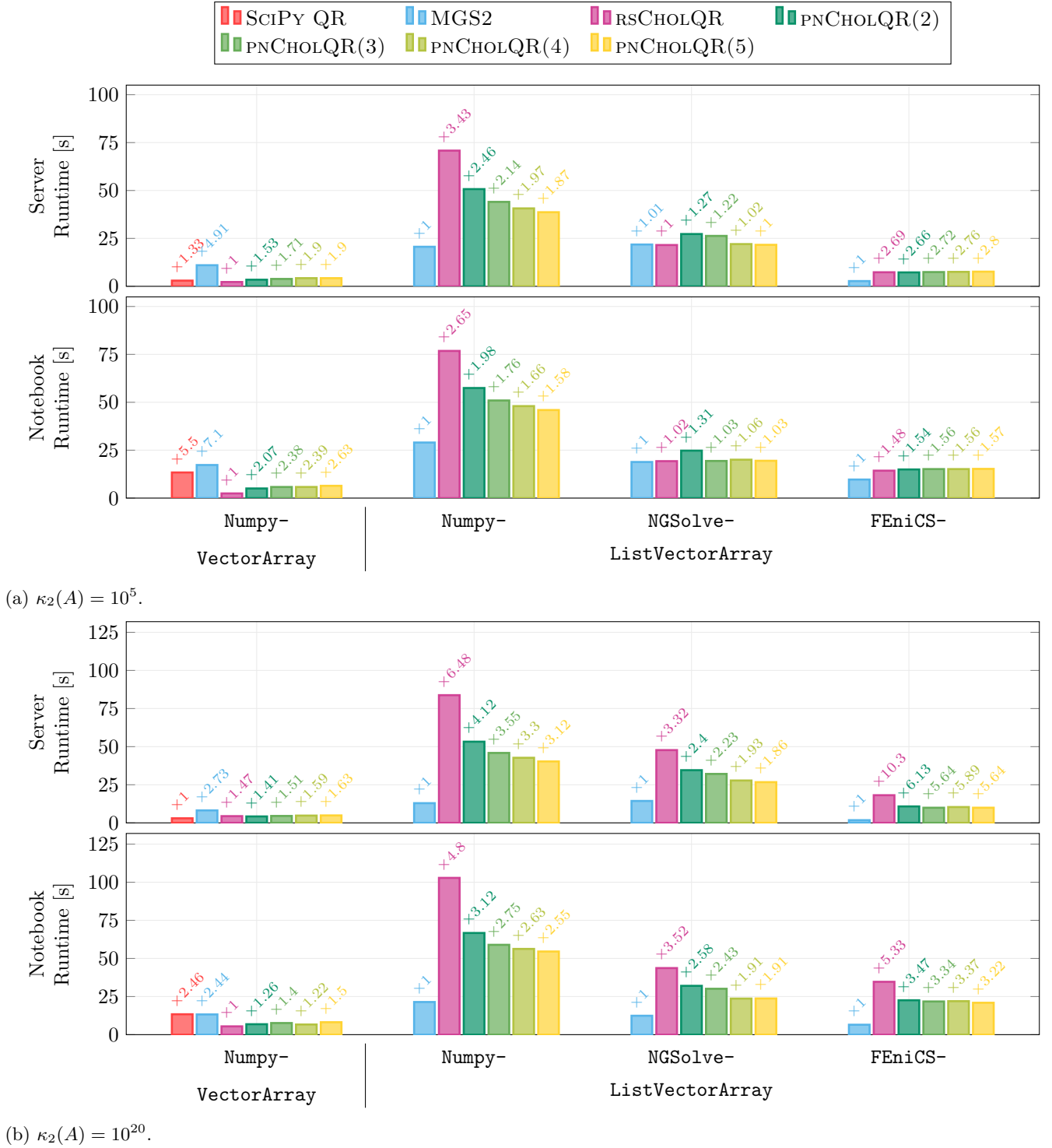


Figure 5: Runtime over varying `VectorArray` backends with 10 repetitions,  $A \in \mathbb{R}^{10^6 \times 100}$ . SciPy QR is shown in the category `NumpyVectorArray`, but works on a `numpy.ndarray`.

is a wrapper for the LAPACK routines `xGEQRF` and `x(OR/UN)GQR`, for comparison as an efficient and readily available function for general Python users. Note that one has to explicitly request `SCIPY QR` to compute an economy size QR decomposition.

4. The algorithms `gram_schmidt` (MGS2) and `shifted_chol_qr` (RSCHOLQR) are part of the `pyMOR` package. Here, MGS2 is a repeated, modified Gram-Schmidt algorithm with additional rank-revealing features. The default settings of the algorithm include a drop-tolerance of  $10^{-13}$  for linearly dependent vectors.

The `shifted_chol_qr` routine is an implementation of Algorithms 1 and 2, whose interface allows switching between both algorithms.

5. Lastly, we used an implementation of Algorithm 3 (PNCHOLQR(R)), which is currently not part of the official `pyMOR` package.

While the algorithms in items 1–3 work on matrices of the datatype `numpy.ndarray`, the latter three algorithms in items 4 & 5 are all implemented based on `pyMOR`'s abstract `VectorArray` interface. In principle, a `VectorArray` is a wrapper for an array of vectors of a given solver backend. Implementations for different backends exist. In this paper, we only focus on the `NumpyVectorArray` and different types of `ListVectorArrays`. A `NumpyVectorArray` is a wrapper for a `numpy.ndarray` and maps the `VectorArray` functions onto `numpy.ndarray` operations. As a result, not all `numpy.ndarray` features can be leveraged, but more block operations than for a `ListVectorArray` are available (see below). A `ListVectorArray` is, as the name suggests, simply an abstract list of vectors from a solver backend. We choose to consider vectors from `NumPy` [14], `FEniCS` [1, 29], and `NGSolve` [33, 38] in our measurements. For clarification, a `NumpyVectorArray` allows us to use many BLAS level-3-type routines while a `NumpyListVectorArray` can only operate vector-vector-wise, i.e., only BLAS level-1-type routines. The latter also applies to all other `ListVectorArrays`.

It is important to note that our implementations of `RSCHOLQR` and `PNCHOLQR(R)` utilize `VectorArrays` for the matrices associated with  $A$  and  $Q$ , only. All other matrices, i.e.,  $R, B, X$  and  $I$ , are assumed to be small enough and stored as `numpy.ndarrays` for which we can use BLAS and LAPACK routines.

Furthermore, algorithms `ITER-SCHOLQR`, `RSCHOLQR` and `PNCHOLQR(R)` all have a stopping criterion of

$$\|I - Q^T Q\|_F \leq 10^{-13},$$

and we allow a maximum of 10 iterations (outer iterations for the `PNCHOLQR(R)`). Also, all employed algorithms work on a copy of the input matrix rather than in-place, since we are not able to exclude the copy time of the `SCIPY QR` function.

We generate our test matrices  $A$  pseudo-randomly via a commonly found SVD approach ( $A := U\Sigma V$ ). Hereby, we construct two random orthogonal matrices  $U \in \mathbb{R}^{m \times n}$ ,  $V \in \mathbb{R}^{n \times n}$  and an ill-conditioned diagonal matrix  $\Sigma \in \mathbb{R}^{n \times n}$ . The values in  $\Sigma$  are log-equidistant starting from 1 up to the desired matrix condition number  $\kappa_2(A) = \frac{\sigma_{\max}}{\sigma_{\min}}$ . The seed used for the pseudo-random number generator is varied with the matrix dimensions and the condition number. The test matrix and all intermediate matrices are of data type IEEE-754 double precision, i.e., 64-bit floating point numbers, hence  $\mathbf{u} \approx 1.11 \cdot 10^{-16}$ .

The following metrics are measured and evaluated:

**Runtime** We measure the wall-time of a QR decomposition call in seconds and evaluate the median of multiple repetitions. The number of repetitions is specified in the caption of each figure.

**Loss of orthogonality**

$$\varepsilon_{\text{LOO}}(Q) = \|I - Q^T Q\|_2$$

**Relative reconstruction residual**

$$\varepsilon_{\text{RRR}}(A, Q, R) = \frac{\|A - QR\|_2}{\|A\|_2}$$

**Relative Cholesky residual**

$$\varepsilon_{\text{RCR}}(A, R) = \frac{\|A^T A - R^T R\|_2}{\|A\|_2^2}$$

### 3.2. An overview of Cholesky QR variants

In this subsection, we perform a comparison between existing Cholesky QR variants and `RSCHOLQR`. We use small matrices of size  $A \in \mathbb{R}^{300 \times 10}$  with ever-increasing matrix condition numbers, mimicking the numerical experiment in [21, Fig. 6.4]. This is done in order to reduce theoretical restrictions on the shift. Prior to conducting the comparison, it is necessary to consider the following aspects and assumptions:

1. Since `RSCHOLQR` is implemented in `pyMOR`, it has a higher overhead due to the additional function layer of the `VectorArray` interface. In order to implement the algorithm, our current implementation additionally requires many delete/copy calls instead of truly working in-place, which degrades the performance further.

2. Given the norm equivalence

$$\|Q^T Q - I_n\|_F \leq \|Q^T Q - I_n\|_2 \leq \sqrt{n} \|Q^T Q - I_n\|_F$$

between the spectral and Frobenius norm and the stopping criterion  $\|Q^T Q - I_n\|_F \leq 10^{-13}$  for `ITER-SCHOLQR` and `RSCHOLQR`. The stopping criterion in spectral norm is bounded from above by

$$\|Q^T Q - I_n\|_2 \leq \sqrt{n} \|Q^T Q - I_n\|_F \approx 3.16 \cdot 10^{-13},$$

which is represented by the red, dashed line in Figure 1b.

3. Numerical results depend on the used hardware and even a use of virtual environments cannot entirely remedy this fact. This phenomenon can be observed by different failing behavior of SCHOLQR3 and ITER-SCHOLQR on the server and notebook for  $\kappa_2(A) \geq 10^{-16}$ . In our case, it might be caused by a different execution order of operations, i.e., error perturbation; e.g., due to a different tiling scheme of the underlying OpenBLAS caused by varying cache sizes or the number of cores available.

A major factor for the success, i.e., a low  $\varepsilon_{\text{LOO}}$ , of Cholesky QR algorithms is the matrix condition number of the input matrix  $A$ , since it is effectively squared for the Gramian  $X = A^T A$ . As a result, the simple CHOLQR has high errors and CHOLQR2 fails to compute the Cholesky decomposition usually for  $\kappa_2(A) \geq \sqrt{\mathbf{u}^{-1}}$ . As can be seen, SCHOLQR3 and ITER-SCHOLQR are numerically robust for  $\kappa_2(A) \leq 10^{15}$ . For even higher condition numbers, they become unreliable and might fail<sup>8</sup>. RSCHOLQR, on the other hand, is able to compute the QR decomposition for matrices with such high condition numbers and that even for larger matrices, as we will see in Sections 3.3 and 3.4. However, this comes at the cost of runtime, since the norm of the Gramian has to be computed potentially multiple times. Again, we would like to point out that the runtime is negatively influenced by the `VectorArray` interface.

### 3.3. Analysis of numerical errors

In Figure 1, we illustrate the numerical robustness of RSCHOLQR and PNCHOLQR( $r$ ) ( $r = 2, \dots, 5$ ). Here, we only show our measurements based on a varying matrix condition number. More quality measures for the variation of different aspects of the original matrix can be found in our repository [8].

Due to the essence of the Cholesky QR algorithms ( $Q := AR^{-1}$ ), we can expect low relative reconstruction residual errors  $\varepsilon_{\text{RRR}}$ . Nonetheless, the orthogonality of  $Q$  is fully dependent on the quality of  $R$ , which explains the importance of including the relative Cholesky residuals  $\varepsilon_{\text{RCR}}$  in our measurements. The errors of the Cholesky QR variants are comparable to SCIPY QR errors.

The increase in  $\varepsilon_{\text{RRR}}$  for MGS2 for high condition numbers is due to its rank-revealing features, which are active by default. Some vectors are linearly dependent, which causes them to be dropped. Therefore, the original matrix  $A$  can only be reconstructed with higher errors. At the same time, this is also the cause for its slight speedup in Figure 3a.

<sup>8</sup>Here, it strongly depends on the seed when SCHOLQR3 and ITER-SCHOLQR fails. We have noticed that for the given test matrix construction and size both of them struggle for  $\kappa_2(A) \geq 10^{16}$

### 3.4. Runtime measurements

In the following we discuss our runtime measurements and illustrate the dependence on a multitude of factors. We investigate the changes in runtime depending on matrix properties like the dimension  $A \in \mathbb{R}^{m \times n}$ , but also the matrix condition number  $\kappa_2(A)$ . Furthermore, as already mentioned, we use two different hardware systems to observe potential differences in the behavior of the algorithms. Also, since this work is done for the pyMOR context, we look into different `VectorArrays`. Due to the limited size of the notebook's main memory, some measurements in Figures 3b and 3c terminate for  $m \geq 10^{6.48}$  and  $n \geq 250$ , respectively.

The main takeaway of Figure 3a is that, in contrast to SCIPY QR, the runtime of the algorithms does not only depend on the matrix dimensions, but depends on the matrix condition number. The runtime of the Cholesky QR variants (RSCHOLQR and PNCHOLQR( $r$ )) increases for higher condition numbers, since more iterations and shift recomputations have to be performed in order to achieve orthogonality. This is important to note, since we use  $\kappa_2(A) = 10^{20}$  in Figures 3b, 3c and 5b. The improved robustness of RSCHOLQR is paid by a factor of 3 and 3.58 in runtime for high condition numbers, compared to low condition numbers on the server and notebook, respectively. Furthermore, PNCHOLQR( $r$ ) has a much steeper increase in runtime for  $\kappa_2(A) \leq 10^4$ , but only slowly increases thereafter. While on the server hardware all competitors are significantly faster than pyMOR's default (MGS2) and of rather similar performance among each other, on the notebook the Cholesky QR variants can even beat the computation times of SCIPY QR by a margin, with our newly suggested RSCHOLQR clearly fastest for all condition numbers.

In Figure 3b, we consider a constant number of vectors ( $n = 100$ ), but vary its length  $m$ . For better visibility, we depict the runtime in relation to  $m$ . Roughly speaking, QR decompositions are of the time complexity class  $\mathcal{O}(mn^2)$ . The resulting line plot can be interpreted as the effective constant of the term  $mn^2$ . As one can see, this constant varies depending on  $m$  (the tall matrix direction). In comparison to the experiments above, SCIPY QR faces more memory management and movement. In particular one can observe this for  $m \geq 10^{4.5}$  on the notebook.

Figure 3c illustrates the runtime over a varying number of vectors  $n$ . Here, PNCHOLQR( $r$ ) scales consecutively worse for an increasing amount of panels  $r$ , where RSCHOLQR, i.e.,  $r = 1$ , has the lowest runtime out of the Cholesky variants. MGS2, being a Gram-Schmidt based algorithm, has a significant increase in runtime for larger  $n$ . Lastly, the runtime of SCIPY QR varies the most between the used hardware. On the server it has consecutively the lowest runtime, but on the notebook it performs even worse than PNCHOLQR(5). However, it is

important to note that the Gramian has an insignificant size in all measurements and fits into the caches, which makes it cheap to work with.

In Figure 4 we repeat the test with a lower condition number  $\kappa_2(A) = 10^5$ , but up to  $n = 10\,000$  vectors. Here, we can observe that up to  $n \leq 3\,500$  the panel variants are similar in runtime to SCIPY QR. RSCHOLQR, on the other hand, performs much better compared to PNCHOLQR(R), due to the reduced condition number (c.f. Figure 3a). Starting with  $n \geq 4\,000$  vectors the panel variants are faster than SCIPY QR and keep a lower increase rate. Note, that the panel variants have an uneven increase in runtime for an increasing amount of vectors. Furthermore, the runtime even decreases in some cases, e.g., PNCHOLQR(5) for  $n = 5\,000$  compared to  $n = 4\,500$ . Note, many numerical solvers, like OpenBLAS, use tiling schemes with powers of two for matrices. Therefore, we suspect, that the size of the Gramians is more suited. PNCHOLQR(R) can be derived to use panels of said sizes. Starting with  $n \geq 9\,000$  vectors, the runtime of RSCHOLQR increases at a considerably higher rate, which might be caused by the amount of data of the Gramian. For more than  $n \geq 10\,000$  vectors, its runtime might even fall above the runtime of PNCHOLQR(R). The L3 caches of the used server have a total size of 256 MB, which means that they are unable to store the full Gramian for  $n \geq 5\,657$ , making it evermore expensive to compute its norm and Cholesky decomposition. However, this is not as visible, since a lower matrix condition number is being used.

In Figures 5a and 5b, we looked into the runtime behavior depending on the `VectorArray` backend. SCIPY QR is shown in the category `NumpyVectorArray` but works on a `numpy.ndarray`. Since the pyMOR algorithms can only work vector-wise with `ListVectorArrays`, we can see a considerable increase in runtime for the Cholesky QR variants. This is due to the overhead in the Gramian construction, which could previously be computed by use of `xGEMM`, i.e., in level-3-type BLAS, and now falls back to level-1-type BLAS. However, here, the panel variants can show their benefits. For the `NumpyListVectorArray` and `NGSolveListVectorArray`, the expected speedup of two (see Appendix A) for an increasing number of panels is approached. Nevertheless, the runtime is larger compared to MGS2. The `FEniCSListVectorArray` implementation, on the other hand, behaves notably different, where more than two panels do not provide a meaningful speedup. However, MGS2 does in fact gain a substantial speedup when using FEniCS. Note however, that the runtime advantage of MGS2 shrinks drastically for moderate condition numbers (Figure 5a) and is most present when many vectors turn out to be linearly dependent ( $\kappa_2(A) = 10^{20} \gg \frac{1}{u}$  in Figure 5b).

## 4. Conclusions and Outlook

Our proposed RSCHOLQR and PNCHOLQR(R) are numerically robust even for high matrix condition numbers (even  $\kappa_2(A) = 10^{20} \gg \frac{1}{u}$ ), making them an improvement compared to SCHOLQR3 and ITER-SCHOLQR, which are working well for  $\kappa_2(A) < \frac{1}{u}$ . Additionally, depending on hardware and matrix properties (condition number and dimensions), they can be faster than SCIPY QR, and a similar advantage is also seen with SCHOLQR3 and ITER-SCHOLQR. Even when using the pyMOR interface, lower runtimes have been observed, suggesting that dedicated reimplementations of these algorithms may be of interest. Since our suggestions seem to be most robust and do not lose too much performance compared to the others, in situations where the condition number is unknown we recommend their use. Whenever expected condition numbers are below  $\frac{1}{u}$ , SCHOLQR3 and ITER-SCHOLQR are still the better choices, and even CHOLQR may be a excellent (and fast) solution for  $\kappa_2(A) < \frac{1}{\sqrt{u}}$ .

However, there are still open questions that may help to improve our algorithmic variants. Regarding the optimal number of panels for PNCHOLQR(R), or the best panel width, respectively. Both depend on the number of vectors  $n$ , additional research is needed. As mentioned before, using a width of a power of two could be beneficial for the used numerical solvers. In theory PNCHOLQR(R) reduces the required flops by up to one half compared to RSCHOLQR, however memory access patterns require closer investigation for the runtime optimization. Better shifting strategies and handling of linear dependencies are also areas for improvement, as they could potentially reduce the number of inner iterations.

Finally, it is worth noting that for the usage with ill-conditioned `VectorArrays` in pyMOR, our Cholesky QR variant is currently only suitable, when used in combination with the `NumpyVectorArray`. Otherwise, the default rank-revealing features of the current repeated modified Gram-Schmidt implementation are presenting an advantage that our current formulations do not have. The use of rank-revealing computations around the Gramian matrices is necessary for which the idea of pivoted Cholesky QR, as proposed in [22], is a promising approach.

## Acknowledgement

The work of Art J. R. Pelling was funded by the Deutsche Forschungsgemeinschaft (DFG, German Research Foundation), project number 504367810. The work of Maximilian Bindhak has been supported by MaRDI, funded by the Deutsche Forschungsgemeinschaft (DFG, German Research Foundation), project number 460135501, NFDI 29/1 “MaRDI – Mathematische Forschungsdateninitiative”.

## References

- [1] M. S. ALNAES, J. BLECHTA, J. HAKE, A. JOHANSSON, B. KEHLET, A. LOGG, C. N. RICHARDSON, J. RING, M. E. ROGNES, AND G. N. WELLS, *The FEniCS project version 1.5*, Archive of Numerical Software, 3 (2015), <https://doi.org/10.11588/ans.2015.100.20553>.
- [2] A. C. ANTOULAS, *Approximation of Large-Scale Dynamical Systems*, Advances in Design and Control, Society for Industrial and Applied Mathematics, Philadelphia, 2005.
- [3] ARPACK-NG CONTRIBUTORS, *ARPACK-NG*, <https://github.com/opencollab/arpack-ng>.
- [4] P. BENNER, A. COHEN, M. OHLBERGER, AND K. WILLCOX, eds., *Model Reduction and Approximation: Theory and Algorithms*, no. 15 in Computational Science and Engineering, Society for Industrial and Applied Mathematics, Philadelphia, 2017, <https://doi.org/10.1137/1.9781611974829>.
- [5] P. BENNER, S. GRIVET-TALOCIA, A. QUARTERONI, G. ROZZA, W. H. A. SCHILDERS, AND L. M. SILVEIRA, eds., *Model Order Reduction. Volume 1: System- and Data-Driven Methods and Algorithms*, De Gruyter, Berlin, 2021, <https://doi.org/10.1515/9783110498967>.
- [6] P. BENNER, S. GRIVET-TALOCIA, A. QUARTERONI, G. ROZZA, W. H. A. SCHILDERS, AND L. M. SILVEIRA, eds., *Model Order Reduction. Volume 2: Snapshot-Based Methods and Algorithms*, De Gruyter, Berlin, 2021, <https://doi.org/10.1515/9783110671490>.
- [7] P. BENNER, S. GRIVET-TALOCIA, A. QUARTERONI, G. ROZZA, W. H. A. SCHILDERS, AND L. M. SILVEIRA, eds., *Model Order Reduction. Volume 3: Applications*, De Gruyter, Berlin, 2021, <https://doi.org/10.1515/9783110499001>.
- [8] M. BINDHAK, *Code and data - Towards an Efficient Shifted Cholesky-QR for Applications in Model Order Reduction using pyMOR*, 2025, <https://doi.org/10.5281/zenodo.15729514>.
- [9] C. BISCHOF AND C. VAN LOAN, *The WY Representation for Products of Householder Matrices*, SIAM J. Sci. Statist. Comput., 8 (1987), pp. s2–s13, <https://doi.org/10.1137/0908009>.
- [10] S. BLACKFORD AND J. DONGARRA, *LAPACK Working Note 41*. <https://netlib.org/lapack/lawnspdf/lawn41.pdf>, June 1999. Version 3.0.
- [11] E. CARSON, K. LUND, Y. MA, AND E. OKTAY, *Reorthogonalized pythagorean variants of block classical Gram-Schmidt*, SIAM J. Matrix Anal. Appl., 46 (2025), pp. 310–340, <https://doi.org/10.1137/24M1658723>.
- [12] E. CARSON, K. LUND, AND M. ROZLOŽNÍK, *The stability of block variants of classical Gram-Schmidt*, SIAM J. Matrix Anal. Appl., 42 (2021), pp. 1365–1380, <https://doi.org/10.1137/21M1394424>.
- [13] E. CARSON, K. LUND, M. ROZLOŽNÍK, AND S. THOMAS, *Block Gram-Schmidt algorithms and their stability properties*, Linear Algebra Appl., 638 (2022), pp. 150–195, <https://doi.org/10.1016/j.laa.2021.12.017>.
- [14] CHARLES R. HARRIS AND K. JARROD MILLMAN AND STÉFAN J. VAN DER WALT AND RALF GOMMERS AND PAULI VIRTANEN AND DAVID COUNAPEAU AND ERIC WIESER AND JULIAN TAYLOR AND SEBASTIAN BERG AND NATHANIEL J. SMITH AND ROBERT KERN AND MATTI PICUS AND STEPHAN HOYER AND MARTEN H. VAN KERKWIJK AND MATTHEW BRETT AND ALLAN HALDANE AND JAIME FERNÁNDEZ DEL RÍO AND MARK WIEBE AND PEARU PETERSON AND PIERRE GÉRARD-MARCHANT AND KEVIN SHEPPARD AND TYLER REDDY AND WARREN WECKESSER AND HAMEER ABBASI AND CHRISTOPH GOHLKE AND TRAVIS E. OLIPHANT, *Array programming with NumPy*, Nature, 585 (2020), pp. 357–362, <https://doi.org/10.1038/s41586-020-2649-2>.
- [15] S. CHELLAPPA, *A posteriori Error Estimation and Adaptivity for Model Order Reduction of Large-Scale Systems*, Dissertation, Otto-von-Guericke-Universität, Magdeburg, Germany, 2022, <https://doi.org/10.25673/101396>.
- [16] CONDA CONTRIBUTORS, *conda: A system-level, binary package and environment manager running on all major operating systems and platforms.*, <https://github.com/conda/conda>.
- [17] J. DEMMEL, L. GRIGORI, M. HOEMMEN, AND J. LANGOU, *Communication-optimal parallel and sequential QR and LU factorizations*, SIAM J. Sci. Comput., 34 (2012), pp. A206–A239, <https://doi.org/10.1137/080731992>.
- [18] R. W. FREUND, *Model reduction methods based on Krylov subspaces*, Acta Numer., 12 (2003), pp. 267–319, <https://doi.org/10.1017/S0962492902000120>.
- [19] R. FRITZE, S. RAVE, F. SCHINDLER, P. MLINARIĆ, L. BALICKI, AND H. KLEIKAMP, *pyMOR*, Dec. 2024, <https://doi.org/10.5281/zenodo.14536112>.

- [20] T. FUKAYA, *An investigation into the impact of the structured QR kernel on the overall performance of the TSQR algorithm*, in Proceedings of the International Conference on High Performance Computing in Asia-Pacific Region, HPCAsia '19, New York, NY, USA, 2019, Association for Computing Machinery, p. 81–90, <https://doi.org/10.1145/3293320.3293327>.
- [21] T. FUKAYA, R. KANNAN, Y. NAKATSUKASA, Y. YAMAMOTO, AND Y. YANAGISAWA, *Shifted Cholesky QR for Computing the QR Factorization of Ill-Conditioned Matrices*, SIAM J. Sci. Comput., 42 (2020), pp. A477–A503, <https://doi.org/10.1137/18M1218212>.
- [22] T. FUKAYA, Y. NAKATSUKASA, AND Y. YAMAMOTO, *A Cholesky QR type algorithm for computing tall-skinny QR factorization with column pivoting*, in 2024 IEEE International Parallel and Distributed Processing Symposium (IPDPS), IEEE, May 2024, pp. 63–75, <https://doi.org/10.1109/IPDPS57955.2024.00015>.
- [23] T. FUKAYA, Y. NAKATSUKASA, Y. YANAGISAWA, AND Y. YAMAMOTO, *CholeskyQR2: A Simple and Communication-Avoiding Algorithm for Computing a Tall-Skinny QR Factorization on a Large-Scale Parallel System*, in 2014 5th Workshop on Latest Advances in Scalable Algorithms for Large-Scale Systems, New Orleans, LA, USA, Nov. 2014, IEEE, pp. 31–38, <https://doi.org/10.1109/Scala.2014.11>.
- [24] G. H. GOLUB AND C. F. VAN LOAN, *Matrix Computations*, Johns Hopkins Studies in the Mathematical Sciences, Johns Hopkins University Press, Baltimore, fourth ed., 2013.
- [25] E. J. GRIMME, *Krylov projection methods for model reduction*, Ph.D. Thesis, Univ. of Illinois at Urbana-Champaign, USA, 1997, <https://perso.uclouvain.be/paul.vandooren/ThesisGrimme.pdf>.
- [26] S. GUGERCIN, A. C. ANTOULAS, AND C. BEATTIE, *H2 Model Reduction for Large-Scale Linear Dynamical Systems*, SIAM J. Matrix Anal. Appl., 30 (2008), pp. 609–638, <https://doi.org/10.1137/060666123>.
- [27] C. LANCZOS, *An iteration method for the solution of the eigenvalue problem of linear differential and integral operators*, J. Research Nat. Bur. Standards, 45 (1950), pp. 255–282.
- [28] R. B. LEHOUCQ, D. C. SORENSSEN, AND C. YANG, *ARPACK Users' Guide*, Society for Industrial and Applied Mathematics, 1998, <https://doi.org/10.1137/1.9780898719628>.
- [29] A. LOGG, K.-A. MARDAL, G. N. WELLS, ET AL., *Automated Solution of Differential Equations by the Finite Element Method*, Springer, 2012, <https://doi.org/10.1007/978-3-642-23099-8>.
- [30] R. MILK, S. RAVE, AND F. SCHINDLER, *pyMOR – Generic Algorithms and Interfaces for Model Order Reduction*, SIAM J. Sci. Comput., 38 (2016), pp. S194–S216, <https://doi.org/10.1137/15M1026614>.
- [31] MINIFORGE CONTRIBUTORS, *Miniforge*, <https://github.com/conda-forge/miniforge>.
- [32] R. MINSTER, A. K. SAIBABA, J. KAR, AND A. CHAKRABORTTY, *Efficient Algorithms for Eigen-system Realization Using Randomized SVD*, SIAM J. Matrix Anal. Appl., 42 (2021), pp. 1045–1072, <https://doi.org/10.1137/20M1327616>.
- [33] NGSOLVE CONTRIBUTORS, *NGSolve*, <https://github.com/NGSolve/ngsolve>.
- [34] OPENBLAS CONTRIBUTORS, *OpenBLAS*, <https://github.com/OpenMathLib/OpenBLAS>.
- [35] A. J. R. PELLING AND E. SARRADJ, *Adaptive Reduced Order Modelling of Discrete-Time Systems with Input-Output Dead Time*, arXiv.org, (2025), <https://arxiv.org/abs/2506.08870>.
- [36] PYMOR DEVELOPERS AND CONTRIBUTORS., *pyMOR – Model Order Reduction with Python*, <https://pymor.org>.
- [37] J. SAAK, *Efficient Numerical Solution of Large Scale Algebraic Matrix Equations in PDE Control and Model Order Reduction*, Dissertation, Technische Universität Chemnitz, Chemnitz, Germany, July 2009, <http://nbn-resolving.de/urn:nbn:de:bsz:ch1-200901642>.
- [38] SCHÖBERL, JOACHIM, *NETGEN an advancing front 2D/3D-mesh generator based on abstract rules*, Computing and Visualization in Science, 1 (1997), pp. 41–52.
- [39] R. SCHREIBER AND C. VAN LOAN, *A Storage-Efficient \$WY\$ Representation for Products of Householder Transformations*, SIAM J. Sci. Statist. Comput., 10 (1989), pp. 53–57, <https://doi.org/10.1137/0910005>.
- [40] L. SIROVICH, *Turbulence and the dynamics of coherent structures. parts I-III*, Quart. Appl. Math., 45 (1987), pp. 561–590, <http://www.jstor.org/stable/43637457>.
- [41] D. C. SORENSSEN, *Implicitly Restarted Arnoldi/Lanczos Methods for Large Scale*



*Eigenvalue Calculations*, Springer Netherlands, Dordrecht, 1997, pp. 119–165, [https://doi.org/10.1007/978-94-011-5412-3\\_5](https://doi.org/10.1007/978-94-011-5412-3_5).

- [42] L. N. TREFETHEN AND D. BAU, III, *Chapter II: QR Factorization and Least Squares*, in Numerical Linear Algebra, Other Titles in Applied Mathematics, Society for Industrial and Applied Mathematics, Jan. 1997, pp. 41–85, <https://doi.org/10.1137/1.9780898719574.ch2>.
- [43] P. VIRTANEN, R. GOMMERS, T. E. OLIPHANT, M. HABERLAND, T. REDDY, D. COURNAPEAU, E. BUROVSKI, P. PETERSON, W. WECKESSER, J. BRIGHT, S. J. VAN DER WALT, M. BRETT, J. WILSON, K. J. MILLMAN, N. MAYOROV, A. R. J. NELSON, E. JONES, R. KERN, E. LARSON, C. J. CAREY, İ. POLAT, Y. FENG, E. W. MOORE, J. VANDERPLAS, D. LAXALDE, J. PERKTOLD, R. CIMRMAN, I. HENRIKSEN, E. A. QUINTERO, C. R. HARRIS, A. M. ARCHIBALD, A. H. RIBEIRO, F. PEDREGOSA, P. VAN MULBREGT, AND SciPy 1.0 CONTRIBUTORS, *SciPy 1.0: Fundamental Algorithms for Scientific Computing in Python*, Nature Methods, 17 (2020), pp. 261–272, <https://doi.org/10.1038/s41592-019-0686-2>.

## A. Number of Floating Point Operations Evaluation

In the following section we want to provide an overview of how many floating point operations an operation or routine requires. Only the number of additions and multiplications are listed. In the following we use BLAS and LAPACK style routine names for some operations. The routines are to represent the cost of the related operation. The flop count of these routines is documented in LAPACK Working Note 41 [10]. In Table 3 the following matrix definitions are being used:  $A \in \mathbb{R}^{n \times n}$ ,  $B \in \mathbb{R}^{i \times j}$ ,  $C \in \mathbb{R}^{j \times k}$ , upper triangular  $R \in \mathbb{R}^{j \times j}$ , symmetric  $X \in \mathbb{R}^{n \times n}$ .

Due to the limitations of the pyMOR interface, it is not possible to evaluate  $X := Q^T Q$  using the BLAS routine `x(SY/HE)RK`. Furthermore, we also cannot evaluate  $Q := AR^{-1}$  using `xTRMM` for the multiplication with  $R^{-1}$  or `xTRSM` for directly solving the equation. In our implementations, for both cases, we use `xGEMM` indirectly. We evaluated the following flop count based on `xGEMM`.

In `RSCHOLQR`, `CHOLQRUPDATE` and `PNCHOLQR(R)`, we compute the spectral norm of the shift

$$11(mn + n(n+1))\mathbf{u} \|X\|_2$$

by use of the symmetric eigenvalue solver routine `eigsh`, from `scipy.linalg`, which uses the Implicitly Restarted Lanczos Method (IRLM) from ARPACK-NG [3] internally.

```
norm = scipy.sparse.linalg.eigsh(
    X,
    k=1,
    tol=1e-2,
    return_eigenvectors=False,
    v0=np.ones([n])
)[0]
```

Listing 1: Used paramters for the `eigsh` function call.

The used parameters for the function call are documented in Listing 1. For the Cholesky QR we are only interested in the largest eigenvalue, which is why we set `k=1`. Furthermore, we only need a rough approximation of the eigenvalue, so setting `tol=1e-2` reduces the runtime of the routine.

Chapter 2.3.6 of the ARPACK manual [28] states that approximately  $(ncv - nev) \cdot \text{cost matrix-vector-product} = (ncv - nev) \cdot 2n^2$  plus an additional  $4n \cdot ncv(ncv - nev)$  flops are required for the IRLM method. Here, `ncv` and `nev` mean, respectively, the number of Lanczos basis vectors that are being used through the course of the computation and the number of eigenvalues that are to be computed. Looking into the SciPy source code one can find that `ncv` is evaluated to be `ncv = min(n, max(2k + 1, 20)) = min(n, 20)`. Therefore, approximately  $38n^2 + 1520n = \mathcal{O}(n^2)$  flops are required to compute the largest eigenvalue.

### A.1. Number of flops comparison between `rsCholQR` and `pnCholQR(r)`

Given  $A \in \mathbb{R}^{m \times n}$ ,  $0 < r \leq n$  such that  $\frac{n}{r} = p$ ,  $r, p \in \mathbb{N}_{>0}$ . Under the assumption that all outer and inner loops of a `CHOLQRUPDATE` call require  $x$  and  $y$  iterations respectively. For simplification, we consider the case where  $n^3 \ll m$ , which means that only terms with the variable  $m$  are relevant for the comparison.

$$G(r) = \lim_{n \rightarrow \infty} F(r) \quad (0 \leq x < \infty)$$

$$= \frac{1}{2} + \frac{1}{2r} \quad (1)$$

In Equation (1) one can see, that for large enough  $n$  the term  $\frac{x}{4nx+2n}$  becomes insignificant. Furthermore, the function  $G(r)$  approaches  $\frac{1}{2}$  asymptotically for an increasing amount of panels, i.e., `PNCHOLQR(N)` requires half as many flops as `RSCHOLQR`. Intuitively, `PNCHOLQR(1)` require as many flops as `RSCHOLQR`.

Operation	Routine	Number Operations
$B \cdot C$	<code>xGEMM</code>	$2ijk$
$B \cdot R$	<code>xTRMM</code> (Mult. with $R$ from the right)	$ij^2$
$R \cdot C$	<code>xTRMM</code> (Mult. with $R$ from the left)	$kj^2$
$\text{chol}(A)$	<code>xPOTRF</code>	$\frac{1}{3}n^3 + \frac{1}{2}n^2 + \frac{1}{6}n$
$\text{inv}(R)$	<code>xTRTRI</code>	$\frac{1}{3}n^3 + \frac{2}{3}n$
$\ X\ _2$	<code>scipy.linalg.eigsh</code>	$\mathcal{O}(n^2)$
$\ A\ _F$	<code>scipy.linalg.norm(X, ord='fro')</code>	$2n^2 + n$

Table 3: FLOP count of used routines.

Line	Routine	Number Operations
3	<code>xGEMM</code>	$2mn^2$
4	<code>scipy.linalg.norm</code>	$(x+1) \cdot [2n^2 + n]$
5	<code>xPOTRF</code>	$x \cdot [\frac{1}{3}n^3 + \frac{1}{2}n^2 + \frac{1}{6}n]$
6	<code>scipy.linalg.eigsh</code>	$x \cdot \mathcal{O}(n^2)$
7	<code>xPOTRF</code>	$x \cdot [\frac{1}{3}n^3 + \frac{1}{2}n^2 + \frac{1}{6}n + n]$
9	<code>xTRTRI</code> + <code>xGEMM</code>	$x \cdot [\frac{1}{3}n^3 + \frac{2}{3}n + 2mn^2]$
10	<code>xTRMM</code>	$x \cdot n^3$
11	<code>xGEMM</code>	$x \cdot 2mn^2$
Total:		$= 2mn^2 + 2n^2 + n$
		$+ x \cdot [4mn^2 + 2n^3 + 3n^2 + \mathcal{O}(n^2) + 3n]$

Table 4: Operation count for RSCHOLQR as defined in Algorithm 1. Under the assumption that the outer loop iterates  $x$  times (condition is evaluated  $x+1$  times).

Line	Routine	Number Operations
4	<code>xGEMM</code>	$2mqp$
5	2 <code>xGEMM</code>	$2mp^2 + 2qp^2 + p^2$
6	<code>scipy.linalg.norm</code>	$(x+1) \cdot [2p^2 + p]$
8	<code>xPOTRF</code>	$x \cdot (y+1) [\frac{1}{3}p^3 + \frac{1}{2}p^2 + \frac{7}{6}p]$
9	<code>scipy.linalg.eigsh</code>	$x \cdot [\mathcal{O}(p^2) + y - 1]$
12	2 <code>xGEMM</code> + <code>xTRTRI</code>	$x \cdot [2mp^2 + 2mqp + mp + \frac{1}{3}p^3 + \frac{2}{3}p]$
13	<code>xGEMM</code>	$x \cdot [2qp^2 + qp]$
14	<code>xTRMM</code>	$x \cdot p^3$
15	<code>xGEMM</code>	$x \cdot 2mqp$
16	2 <code>xGEMM</code>	$x \cdot [2mp^2 + 2qp^2 + p^2]$
Total:		$= 2mp^2 + 2mqp + 2qp^2 + 3p^2 + p$
		$+ x \cdot [4mp^2 + 4mqp + mp + \frac{5}{3}p^3 + 4qp^2 + \frac{7}{2}p^2 + \mathcal{O}(p^2) + qp + \frac{17}{6}p - 1]$
		$+ (y_1 + \dots + y_x) \cdot [\frac{1}{3}p^3 + \frac{1}{2}p^2 + \frac{7}{6}p + 1]$

Table 5: Operation count for CHOLQRUPDATE as defined in Algorithm 2. Under the assumption that the outer loop iterates  $x$  times (condition is evaluated  $x+1$  times) and that the inner loop iterates  $y_1, y_2, \dots, y_x$  times (condition is evaluated  $y+1$  times).

	Number Operations
Total:	$= mn^2 + \frac{mn^2}{r} + \frac{n^3}{r} - \frac{n^3}{r^2} + \frac{3n^2}{r} + n$
	$+x \cdot \left[ 2mn^2 + \frac{2mn^2}{r} + mn + \frac{2n^3}{r} - \frac{n^3}{3r^2} + \frac{n^2}{2} + \frac{3n^2}{r} + \mathcal{O}\left(\frac{n^2}{r}\right) + \frac{17n}{6} - r \right]$
	$+xy \cdot \left[ \frac{n^3}{3r^2} + \frac{n^2}{2r} + \frac{7n}{6} + r \right]$

Table 6: Operation count for PNCHOLQR(R) as defined in Algorithm 3. Given  $A \in \mathbb{R}^{m \times n}$ ,  $0 < r \leq n$  such that  $\frac{n}{r} = p$ ,  $r, p \in \mathbb{N}_{>0}$ . Under the assumption that all outer and inner loops of a CHOLQRUPDATE call require  $x$  and  $y$  iterations respectively. The assumption onto  $x$  and  $y$  is very pessimistic. In practice, the first few panels might require none or only a few repetitions. The last few panels, on the other hand, require many more repetitions. Furthermore, in terms of flops a failed Cholesky decomposition is counted as a full decomposition.

	Number Operations
PNCHOLQR(R)	$mn^2 + \frac{1}{r}mn^2 + x \cdot \left[ 2mn^2 + \frac{2}{r}mn^2 + mn \right]$
RSCHOLQR	$2mn^2 + x \cdot 4mn^2$
$F(r) = \text{PNCHOLQR(R)} / \text{RSCHOLQR}$	$\frac{1}{2} + \frac{1}{2r} + \frac{x}{4nx+2n}$

Table 7: Operation count ratio between RSCHOLQR and PNCHOLQR(R).